

Very Low-Resolution Iris Recognition Via Eigen-Patch Super-Resolution and Matcher Fusion

Fernando Alonso-Fernandez
IS-Lab/CAISR
Halmstad University (Sweden)
feralo@hh.se

Reuben A. Farrugia
Department of CCE
University of Malta (Malta)
reuben.farrugia@um.edu.mt

Josef Bigun
IS-Lab/CAISR
Halmstad University (Sweden)
josef.bigun@hh.se

Abstract

Current research in iris recognition is moving towards enabling more relaxed acquisition conditions. This has effects on the quality of acquired images, with low resolution being a predominant issue. Here, we evaluate a super-resolution algorithm used to reconstruct iris images based on Eigen-transformation of local image patches. Each patch is reconstructed separately, allowing better quality of enhanced images by preserving local information. Contrast enhancement is used to improve the reconstruction quality, while matcher fusion has been adopted to improve iris recognition performance. We validate the system using a database of 1,872 near-infrared iris images. The presented approach is superior to bilinear or bicubic interpolation, especially at lower resolutions, and the fusion of the two systems pushes the EER to below 5% for down-sampling factors up to a image size of only 13×13 .

1. Introduction

Iris is regarded as the most reliable biometric modality [11]. Current research trends move towards more relaxed acquisition conditions, allowing ‘at a distance’ and ‘on the move’ capabilities [12]. However, this has implications in terms of quality of acquired images, with the lack of pixel resolution being one of the most evident. This paper is concerned with the task of up-sampling, or increasing both size and quality of a low-resolution image as a result, for example, of long acquisition distances. Another piece of research, not addressed here, is concerned with compressed images but with image dimensions kept constant [21].

The aim of super-resolution (SR) techniques is to reconstruct the missing high resolution (HR) image \bar{Y} given a low resolution (LR) image \bar{X} . The LR image is modeled as the corresponding HR image manipulated by blurring B , warping W and down-sampling D (plus some additive noise \bar{n}) as $\bar{X} = DBW\bar{Y} + \bar{n}$. For simplicity, some works omit

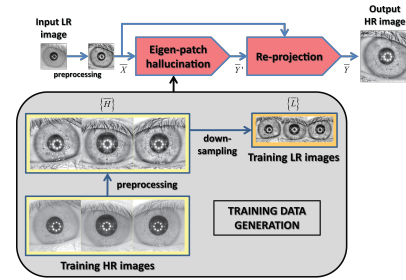


Figure 1. Eigen-patch iris hallucination system.

the warp matrix and noise, leading to $\bar{X} = DB\bar{Y}$. Super-resolution can enhance the quality of LR images, and thus the recognition performance. However, SR in biometrics is relatively recent, with a lot of research in face since 2002 (also called hallucination) [26], and a much more limited amount for iris and ocular modalities. Despite the vast literature on image SR, one reason of such limited research might be that most SR approaches are general-scene, designed to produce overall visual enhancement, but the aim of biometrics is a better recognition accuracy [18]. Therefore, adaptation of super-resolution techniques to the particularities of images from a specific biometric modality is needed to achieve a more efficient up-sampling [4]. Two main SR approaches exist: reconstruction- and learning-based [20]. In reconstruction-based, multiple LR images are fused to obtain a HR image, therefore several LR images are needed as input (which might not always be the case). Alternatively, learning-based methods model the relationship between LR and HR images with a training dictionary, using the learned model to up-sample unseen LR images. Learning-based methods only need one LR image as input, and generally outperform reconstruction-based methods, achieving higher magnification factors [20]. The few works available on iris learning-based approaches employ Multi-Layer Perceptrons [23], or frequency analysis [9]. One major limitation is that they try to develop a prototype iris using combination of complete images. Eigen-patches

is a strategy which models a local patch using collocated patches from a dictionary, instead of using the whole image. Each patch is hallucinated separately, providing better quality reconstructed prototypes with better local detail and lower distortions. Local methods are also generally superior in recovering texture than global methods, which is essential due to the prevalence of texture-based methods in ocular biometrics [19].

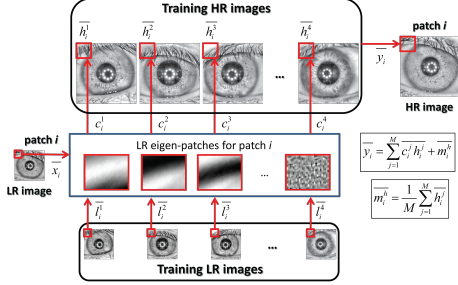


Figure 2. Eigen-patch hallucination step.



Figure 3. Example of images of the CASIA Interval v3 database with the annotated circles modeling iris boundaries and eyelids.

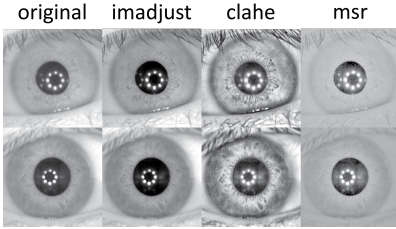


Figure 4. Example of HR original images with different contrast enhancement techniques.

In this paper, we apply an iris super-resolution technique based on PCA Eigen-transformation of local image patches inspired by the system of [7] for face images. A PCA Eigen-transformation is conducted in each patch of the input LR image. The HR patch is then reconstructed as a linear combination of collocated HR patches of the training database. This way, every patch has its own optimal reconstruction coefficients, allowing to preserve local image information. Prior to the hallucination process, iris images are aligned with respect to the pupil center, since alignment is critical for the performance of SR systems. Despite the patch-based SR approach used is not new, we contribute with its implementation to iris images, and particularly with the application (and fusion) of two iris matchers to the reconstructed images. We also test different global and local contrast enhancement techniques, previously used in iris or face stud-

ies, before carrying out image reconstruction. In our experiments, we employ the CASIA-IrisV3-Interval database [6] of NIR iris images. We conduct verification experiments with two iris matchers based on Log-Gabor wavelets [17] and SIFT keypoints [16]. Log-Gabor exploit texture information globally (across the entire iris image), while SIFT exploit local features (in discrete key points), therefore our motivation is to employ features that are diverse in nature, and reveal if they behave differently. The presented hallucination method is superior to bilinear and bicubic interpolations, with better recognition rates as image resolution decreases. Regarding image enhancement, one of the matchers (SIFT) is benefited by the use of some contrast enhancement before up-sampling, whereas the LG matcher works better without any kind of pre-processing. This is also exploited in the fusion of the two systems, since better fusion results are obtained if images used with each matcher have applied its *optimum* enhancement. In our experiments, performance of the fusion can be pushed to a EER below 5% for any given down-sampling factor (which in this paper includes images of only 13×13). In addition, we observe that recognition performance is not degraded significantly with any matcher until a down-sampling factor of 8 (image size of 29×29). This allows for example to reduce storage or data transmission requirements, and it contributes to the feasibility of 'at-a-distance' iris acquisition as well, which is one of the most important issues for these technologies to achieve massive adoption [12].

2. Iris Hallucination Procedure

The structure of the hallucination method is shown in Figure 1. It is based on the eigen-patch hallucination method for face images of [7]. The system is described next.

2.1. Eigen-Patch Hallucination

Given an input low resolution (LR) iris image \bar{X} , it is first preprocessed to enhance contrast; then, it is separated into N overlapping patches $\{\bar{x}\} = \{\bar{x}_1, \bar{x}_2, \dots, \bar{x}_N\}$. Two super sets of basis patches are computed for each LR patch \bar{x}_i , separate from the input image \bar{X} , from collocated patches of a training database of high resolution images $\{\bar{H}\}$. One of the super sets, $\{\bar{h}_i^1, \bar{h}_i^2, \dots, \bar{h}_i^M\}$, is obtained from collocated (HR) patches. By degradation (low-pass filtering and down-sampling) a low resolution database $\{\bar{L}\}$ is obtained from $\{\bar{H}\}$, and the other super set, $\{\bar{l}_i^1, \bar{l}_i^2, \dots, \bar{l}_i^M\}$, is obtained similarly, but for $\{\bar{L}\}$. M is the size (number of images) of the training set. The same contrast enhancement procedure is applied to the HR iris images of the training set before down-sampling. A PCA Eigen-transformation is then conducted in each input LR patch \bar{x}_i using the collocated patches $\{\bar{l}_i^1, \bar{l}_i^2, \dots, \bar{l}_i^M\}$ of

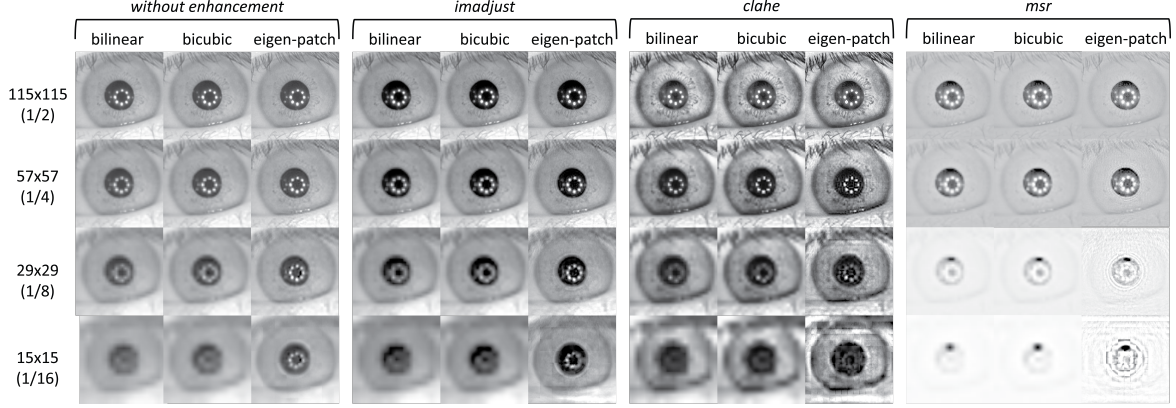


Figure 5. Resulting HR hallucinated images for different down-sampling factors. The original HR images are shown in Figure 4 (first row).

the LR training images to obtain the optimal reconstruction weights $\bar{c}_i = \{c_i^1, c_i^2, \dots, c_i^M\}$ of each patch (see Figure 2). By allowing each LR patch of the input image to have its own optimal reconstruction weights, the HR patch will be closer to the input LR patch, therefore more local information can be preserved and less reconstruction artifacts appear. Once the reconstruction weights \bar{c}_i of each patch are obtained, the HR patches are rendered using the collocated patches of the HR images of the training set $\{\bar{H}\}$. The reconstruction coefficients of the input image \bar{X} using the LR patches is carried on to weight the HR basis set, which yields the preliminary reconstructed HR iris image \bar{Y}' , after averaging the overlapping regions. Additional details of this Eigen-transformation procedure can be obtained in [7].

2.2. Image Re-projection

A re-projection step is applied to \bar{Y}' to reduce artifacts and make the output image \bar{Y} more similar to the input LR image \bar{X} . The image \bar{Y}' is re-projected to \bar{X} via $\bar{Y}^{t+1} = \bar{Y}^t - \tau U \left(B \left(D B \bar{Y}^t - \bar{X} \right) \right)$ where U is the up-sampling matrix. The process stops when $|\bar{Y}^{t+1} - \bar{Y}^t| < \epsilon$. Here we use $\tau=0.02$ and $\epsilon = 10^{-5}$.

3. Iris Matchers

We conduct matching experiments of iris images using two different systems based on 1D Log-Gabor filters (LG) [17] and the SIFT operator [16]. In LG, the iris region is first unwrapped to a normalized rectangle of 20×240 pixels using the Daugman's rubber sheet model [8] and next, a 1D Log-Gabor wavelet is applied plus phase binary quantization to 4 levels. Matching between binary vectors is done using the normalized Hamming distance [8], which incorporates noise mask, so only significant bits are used. Rotation is accounted for by shifting the grid of the query image in counter- and clock-wise directions, and selecting the lowest distance, which corresponds to the best match be-

tween two templates. In the SIFT matcher, SIFT key points are directly extracted from the iris region (without unwrapping), and the recognition metric is the number of matched key points, normalized by the average number of detected keypoints in the two images under comparison. The LG implementation is from Libor Masek code [17], using its default parameters (optimized for CASIA images, which we employ here as well). The SIFT method uses a free toolkit for feature extraction and matching¹, with the adaptations described in [3] (particularly, it includes a post-processing step to remove spurious matching points using geometric constraints). The iris region and corresponding noise mask for feature extraction and matching is obtained by manual annotation of the database used, as shown in Figure 3 (more information is provided in the experimental setup).

4. Experimental Framework

We use the CASIA Interval v3 iris database [6] for our experiments. It has 2,655 NIR images of 280×320 pixels from 249 contributors captured in 2 sessions with a close-up iris camera, totalling 396 different eyes (the number of images per contributor and per session is not constant). Manual annotation of this database is available [1, 10], which has been used as input for our experiments. All images of the database are resized via bicubic interpolation to have the same sclera radius (we choose as target radius the average sclera radius $R=105$ of the whole database, given by the groundtruth). Then, images are aligned by extracting a square region of 231×231 around the pupil center (corresponding to about $1.1 \times R$). In case that such extraction is not possible (for example if the eye is close to an image side), the image is discarded. After this procedure, 1,872 images remain, which will be used for our experiments.

The dataset of aligned images has been divided into two sets, a training set comprised of images from the first 116 users ($M=925$ images) used to train the eigen-patch hallu-

¹<http://vision.ucla.edu/vedaldi/code/sift/assets/sift/index.html>

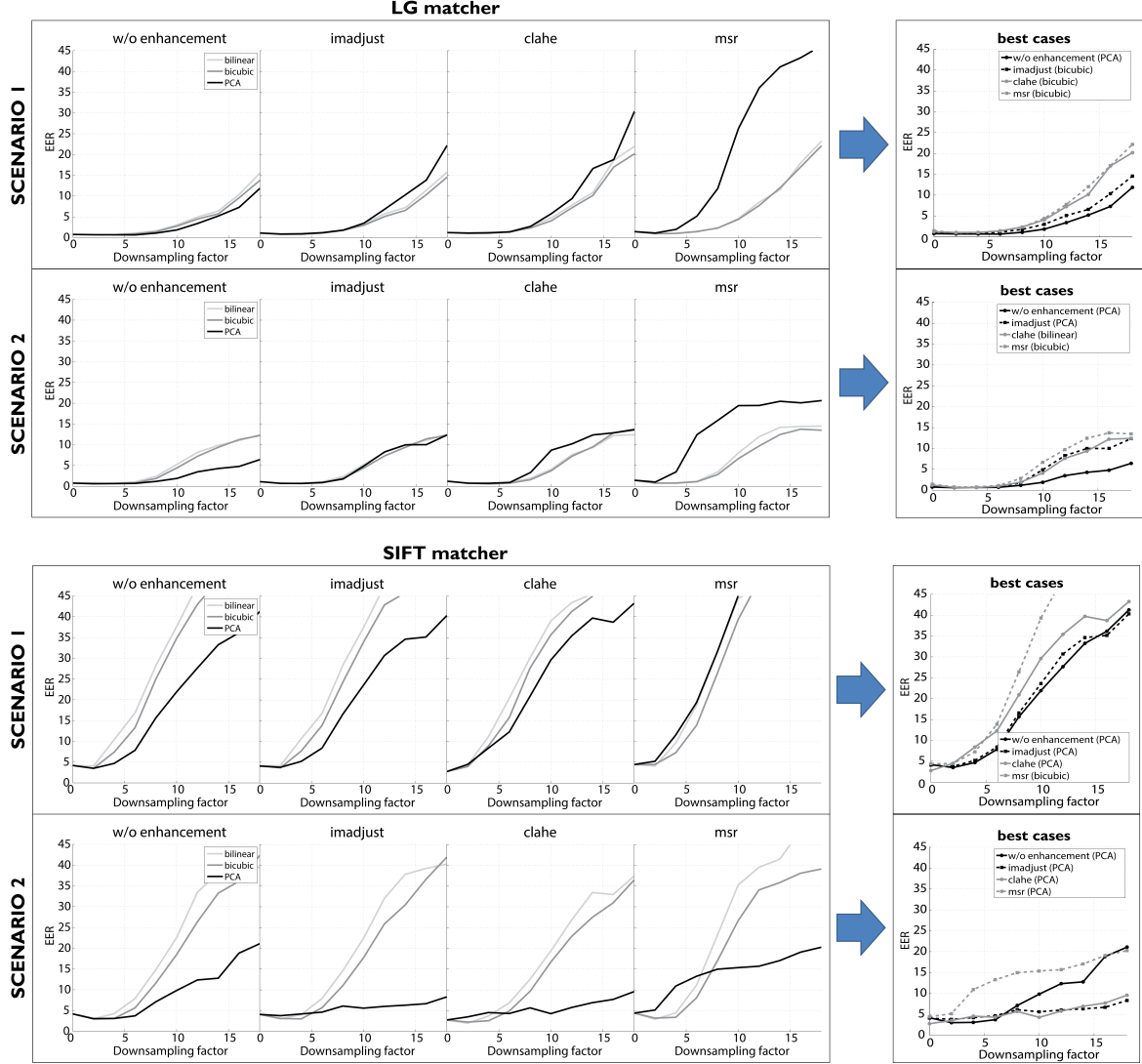


Figure 6. Verification results (EER) of the two scenarios considered with different contrast enhancement techniques.

cination method, and a test set comprised of the remaining 133 users (947 images) which is used for validation. We perform verification experiments with the iris matchers in the test set. We consider each eye as a different user. Genuine matches are obtained by comparing each image of a user to the remaining images of the same user, avoiding symmetric matches. Impostor matches are obtained by comparing the 1st image of a user to the 2nd image of the remaining users. With this procedure, we obtain 2,607 genuine and 19,537 impostor scores.

5. Results

The 947 iris images of the test set are used as our high resolution (HR) reference images. We then down-sample these images via bicubic interpolation by a factor of $2n$ (i.e. the image is resized to $1/(2n)$ of the original HR

size), and the down-sampled images are used as input LR images, from which hallucinated HR images are extracted. This simulated down-sampling is the approach followed in most of the previous super-resolution studies [26], mainly due to the lack of databases with low-resolution and corresponding high-resolution reference images. We test until a down-sampling factor of 18 (corresponding to a LR image size of 13×13). We also extract the normalized iris region (size 20×240) from both the hallucinated HR and the reference HR images, as well as LG and SIFT features, according to the algorithms of Section 3. We compare our method with bicubic and bilinear interpolation as well. Figure 5 shows the hallucinated images (only for a selection of down-sampling factors for the sake of space).

We have tested three different contrast enhancement algorithms with iris images (see Figure 4): mapping of in-

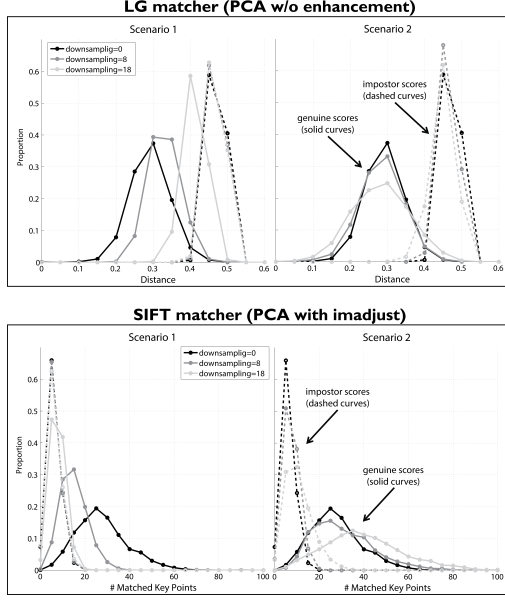


Figure 7. Score distribution of the LG and SIFT matchers for the two scenarios considered (selection of best cases of Figure 6). Results are given for selected down-sampling factors. Solid curves correspond to genuine scores distributions, whereas dashed curves correspond to impostor scores distributions.

tensity values such that 1% of data is saturated at low and high intensities (Matlab command *imadjust*), Contrast-Limited Adaptive Histogram Equalization (*clahe*, with Matlab command *adapthisteq*) [27], and Multi-Scale Retinex (*msr*) [14]. We employ the Multi-Scale Retinex implementation of the INFace (Illumination Normalization techniques for robust Face recognition) toolbox v2.1 [25, 24]. *Imadjust* operates over the whole image, whereas *clahe* and *msr* operate on local image regions or scales. The reasons for our choices is that *clahe* is usually preferred in iris studies over other enhancement methods [22], whereas *msr* has been demonstrated to have superior performance on face images [15]. In our experiments with *clahe*, the number of tiles with HR images are 8×8 (rows \times columns), which are proportionally adjusted for LR images. With *msr*, sizes of the Gaussian smoothing filters are set to 13, 27 and 37 for HR images, which are adjusted proportionally for LR images.

The performance of the hallucination algorithm is measured by reporting verification experiments using hallucinated HR images. We do not report other reconstruction measures traditionally used in super-resolution literature (e.g. PSNR) since the aim of applying SR algorithms in biometrics is enhancing recognition performance [18]. As will be observed here, performance of the two matchers employed is affected in a different way, so even if the reconstruction is ‘good’ (as measured by a general-scene indicator), performance of a matcher may not follow. There-

fore, we believe that focusing on recognition performance is of higher interest. Two scenarios are considered: 1) enrolment samples taken from original HR input images, and query samples from hallucinated HR images; and 2) both enrolment and query samples taken from hallucinated HR images. The first case simulates a controlled enrolment scenario with good quality images, while the second case simulates a totally uncontrolled scenario (albeit for simplicity, enrolment and query samples have similar resolution in our experiments). Results are given in Figure 6. The following observations can be made from these results:

- The performance of the proposed hallucination method is very similar to bilinear and bicubic interpolations for small down-sampling factors, but at low resolutions, the best (smallest) error rates are obtained in general with the proposed eigen-patch hallucination method for both matchers (observe the last column of ‘best cases’ in Figure 6). In addition, when comparing the two matchers, the best absolute performance is given by the LG matcher.
- The performance of both scenarios is similar up to a certain down-sampling factor. However, at low resolutions, the performance of scenario 2 is much better than scenario 1, and this phenomenon is observed with both matchers. We analyze this effect further by plotting in Figure 7 the score distributions of the two matchers for the best cases of Figure 6 (for consistency, results with the SIFT matcher are reported for both scenarios using *imadjust* enhancement). In scenario 1, the distribution of genuine scores is shifted towards the impostor distribution for both matchers as resolution decreases. This means that the ‘similarity’ between hallucinated HR images and original HR images is reduced as the size of input LR images is reduced. In other words, the information recovered by the reconstruction algorithm does not fully resemble the information found in the original HR image (at least measured by the features employed). In scenario 2, the distribution of genuine scores is not significantly shifted as resolution changes, but it tends to be more spread instead. In this case, both gallery and probe images undergo the same down-sampling and up-sampling procedure, therefore they keep more ‘similarity’ in average. A collateral effect of this phenomena however is that the distribution of impostor scores shifts towards the genuine distribution for extreme down-sampling, meaning that hallucinated HR images of different users tend to be more ‘similar’ (under the features used here) as they undergo the mentioned down-sampling and up-sampling procedure.
- The difference in performance between scenario 1 and scenario 2 at low resolutions is much more evident

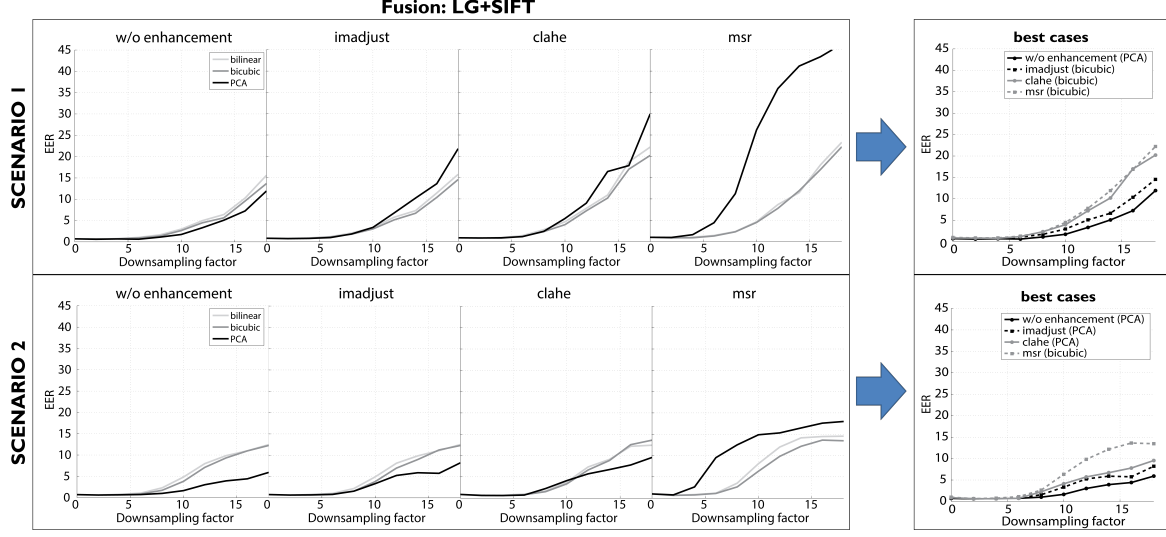


Figure 8. Fusion results (EER) of the two scenarios considered with different contrast enhancement techniques.

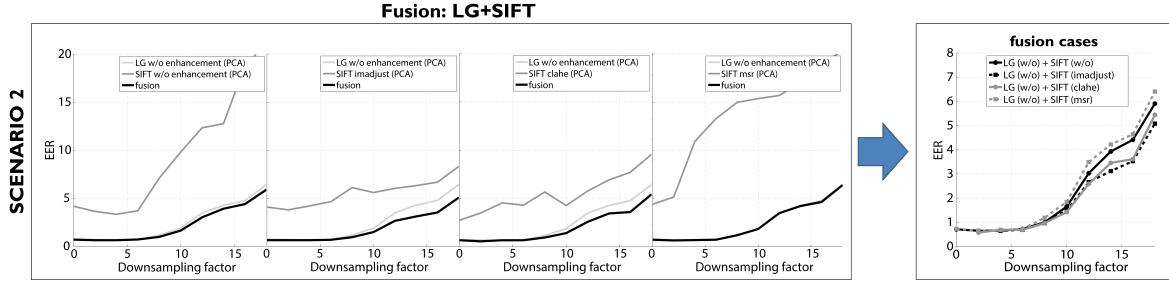


Figure 9. Fusion results (EER) of the LG matcher (without enhancement) and the SIFT matcher (with different enhancements). Results are given for scenario 2 and eigen-patch (PCA) reconstruction only.

with the SIFT matcher: EER in scenario 1 goes above 40% for a down-sampling factor of 18, whereas best EERs in scenario 2 are kept below 10%. With the LG matcher, the best EER in scenario 1 is below $\sim 12\%$, whereas for scenario 2 is below $\sim 6.5\%$. This suggests that the image properties captured by this matcher (using a Log-Gabor wavelet) are less sensitive to changes due to extreme down-sampling. Or seen in a different way, the eigen-patch reconstruction algorithm employed is better in recovering the image properties analyzed by the LG matcher than the image properties analyzed by the SIFT matcher. However, the SIFT matcher is more resilient to reductions in image resolution when operating in scenario 2 (see bottom left plot of Figure 6), with the EER going from 3-4% with no down-sampling to only $\sim 8\%$ with a down-sampling factor of 18. On the other hand, the LG matcher goes from 0.76% to 6.44%, thus increasing EER by an order of magnitude (second plot, last column of Figure 6)

not start to degrade significantly until a down-sampling factor of 8 (image size of 29×29). This is true for the two matchers employed, suggesting that the size of both gallery and probe images can be kept low without sacrificing performance. This has positive implications in terms of low storage or low data transmission needs (original image size is 231×231). With the LG matcher, bilinear and bicubic interpolations show similar performance than the proposed method for small down-sampling factors; however, with the SIFT matcher, bilinear and bicubic interpolations degrade more rapidly than the PCA eigen-patch reconstruction, thus highlighting the benefits of the proposed method even with small down-sampling. It is also remarkable the relatively low EER figures obtained for the most extreme case of down-sampling analyzed here (a factor of 18, which corresponds to an image size of just 13×13): EER of $\sim 6\%$ with the LG matcher and $\sim 8\%$ with the SIFT matcher.

- From the last column of 'best cases' in Figure 6, it can be observed that performance in scenario 2 does
- With regards to the contrast enhancement algorithms employed, they do not benefit the two matchers

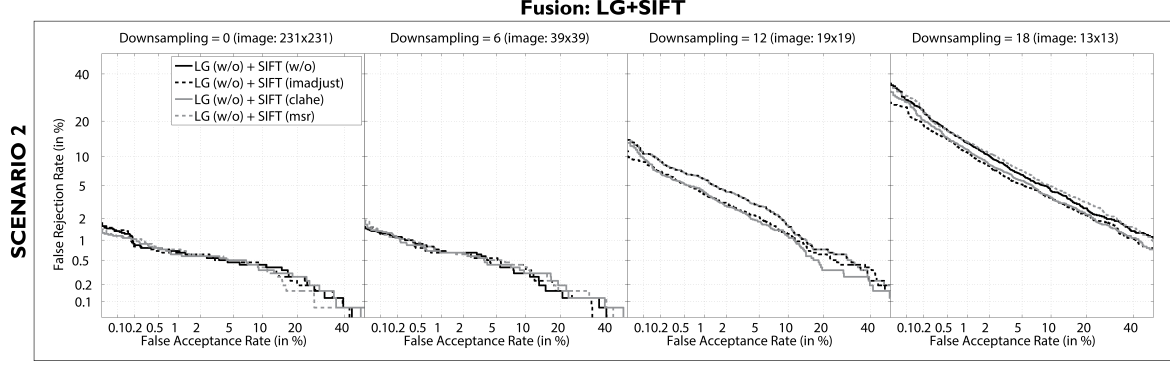


Figure 10. Fusion results (DET curves) of the LG matcher (without enhancement) and the SIFT matcher (with different enhancements) for several selected down-sampling factors. Results are given for scenario 2 and eigen-patch (PCA) reconstruction only.

equally. The best performance with the LG matcher at low resolutions is obtained without any kind of enhancement, but the SIFT matcher is benefited of the use of *imadjust* or *clahe* algorithms. It is of relevance as well that some enhancement techniques produces that bilinear or bicubic interpolations work better than eigen-patch interpolation with the LG matcher (e.g. see *clahe*, which is a popular enhancement algorithm in iris recognition research [22]). There is also consensus in our results on the fact that *msr* produces the worst results with both matchers. It is also worth noting that *imadjust* (which operates over the whole image) and *clahe* (which operates on local patches) result in similar performance with both matchers in scenario 2, see last column of Figure 6.

- Although it is not the scope of this paper, it can be seen in Figure 6 that some curves show a slight improvement in performance after a small down-sampling of just 2 or 4. This suggests that the two matchers used here may benefit of a small image smoothing when using images at the original (high) resolution.

We then carry out fusion experiments using linear logistic regression. Given N matchers ($N=2$ in our case) which output the scores $(s_{1j}, s_{2j}, \dots, s_{Nj})$ for an input trial j , a linear fusion is: $f_j = a_0 + a_1 \cdot s_{1j} + a_2 \cdot s_{2j} + \dots + a_N \cdot s_{Nj}$. The weights a_0, a_1, \dots, a_N are trained via logistic regression as described in [2]. We use this trained fusion approach because it has shown better performance than simple fusion rules (like the mean or the sum rule) in previous works, as in the one reported above. Results are given in Figure 8. Experiments reported in this Figure make use of the same contrast enhancement technique with the two matchers. For this reason, despite the fact that SIFT is benefited by the use of *imadjust* or *clahe*, the best fusion results are obtained without any kind of enhancement, since LG dominates in the fusion due to its smaller individual EER. To counteract this effect, we test several LG+SIFT fusion combina-

tions after applying the different enhancement techniques to the SIFT matcher. Results of this procedure are reported in Figure 9. As it can be observed, better results are obtained at low resolutions when *imadjust* or *clahe* are applied to the SIFT matcher, obtaining higher improvements w.r.t the best individual matcher (i.e. the LG matcher). We also report in Figure 10 the DET curves of the fusion combinations of Figure 9 for several (selected) down-sampling factors. Despite the fact that the EER of the different fusion combinations has been observed to be similar for small down-sampling factors, the leftmost plot of Figure 10 (no down-sampling) suggest that at low FAR or FRR, there is benefit from applying enhancement to the SIFT matcher too (it is even remarkable in this case that at low FRR, the best enhancement is *msr*, which has never appeared as the best option so far). Also, as observed above, the two rightmost plots confirm that *imadjust* or *clahe* should be applied to the SIFT matcher. It is interesting, however, that *imadjust* is more beneficial at low FAR, whereas *clahe* may be preferred at low FRR.

6. Conclusions

The use of more relaxed acquisition conditions will push iris recognition towards the use of low resolution imagery [5]. In this paper, we apply an iris super-resolution technique based on PCA Eigen-transformation of local image patches [7] to increase the resolution of near-infrared (NIR) iris images. We also test the use of different global and local contrast enhancement algorithms with the eigen-patch reconstruction system. The proposed approach is compared to bilinear and bicubic interpolations as well. Performance of the reconstruction algorithm is measured by reporting verification experiments with two iris matchers based on Log-Gabor (LG) wavelets and SIFT keypoints. We consider two operational scenarios, one where original high-resolution images are matched against hallucinated high-resolution images (scenario 1, or controlled enrolment), and another scenario where only hallucinated images are used

(scenario 2, or uncontrolled scenario). Experiments show that, at low resolutions, better performance can be obtained with the proposed eigen-patch reconstruction method w.r.t. bilinear or bicubic interpolation. Regarding image enhancement, the LG matcher shows better performance without any kind of enhancement, whereas the SIFT matcher is benefited by the use of some contrast enhancement before image reconstruction. We also observe that if both gallery and probe images undergo the same down-sampling and up-sampling procedure (scenario 2), they keep more ‘similarity’ than if up-sampled images are matched against original high-resolution images (scenario 1). This is reflected by a better recognition performance of scenario 2 w.r.t. scenario 1 at low resolutions. However, the LG matcher is less sensitive to this effect, as shown by smaller relative differences in performance between the two scenarios than the SIFT matcher. It is also worth noting that performance with any matcher is not significantly degraded until image is down-sampled by 8 or higher factors, allowing to use images of reduced size (of importance for example under low storage or data transmission capabilities). We also perform fusion experiments between the two matchers, with results showing that performance at low resolutions can be further improved, with EER pushed to below 5% for any given down-sampling factor (which in our experiments includes iris images of up to a down-sampling factor of 18, or an image size of only 13×13).

The proposed PCA method assumes linearity in finding the reconstruction weights of each patch; in addition, it employs all available collocated patches of the training database. Allowing non-linearity and deriving an optimal subset of collocated patches from the training set are two avenues that are demonstrating superiority in preserving texture in face super-resolution studies [13], which we will evaluate here too as future work. We expect that these approaches will better cope with artifacts appearing at low resolutions due to division of the image in patches (observe bottom of Figure 5). The latter could be also achieved by exploring other methods to combine overlapping patches during reconstruction. We follow here the predominant approach of averaging patches, which acts as a denoising that reduces texture details and may result in over-smoothing [26], but other approaches should be explored as well. We are also aware of the limitation of comparing our system against simple bilinear and bicubic interpolation approaches. However, as mentioned in the introduction, research in iris super-resolution is limited. Implementation of the improvements mentioned above will lead to the availability of other techniques that will provide a more comprehensive experimental framework. In addition, we have not considered iris reconstruction-based approaches, since they demand more than one image for reconstruction. Another direction is increasing the number of systems involved in

the fusion, as well as the impact of using a smaller training set. We also plan to analyze sensitivity of the proposed method to misalignment of the eye, since alignment is very critical to proper hallucination output.

Acknowledgements

This work was initiated while F. A.-F. was a visiting researcher at the University of Malta, funded by EU COST Action IC1106. Author F. A.-F. also thanks the Swedish Research Council for funding his research, and the CAISR program of the Swedish Knowledge Foundation.

References

- [1] F. Alonso-Fernandez, J. Bigun. Near-infrared and visible-light periocular recognition with gabor features using frequency-adaptive automatic eye detection. *IET Biometrics*, 4(2):74–89, 2015.
- [2] F. Alonso-Fernandez, J. Fierrez, D. Ramos, J. Ortega-Garcia. Dealing With Sensor Interoperability in Multi-biometrics: The UPM Experience at the Biocure Multimodal Evaluation 2007. *Proc BTHI*, 2008.
- [3] F. Alonso-Fernandez, P. Tome-Gonzalez, V. Ruiz-Albacete, J. Ortega-Garcia. Iris recognition based on sift features. *Proc BIDS*, 2009.
- [4] S. Baker and T. Kanade. Limits on super-resolution and how to break them. *IEEE TPAMI*, 24(9):1167–1183, Sep 2002.
- [5] K. Bowyer, K. Hollingsworth, P. Flynn. Image understanding for iris biometrics: a survey. *CVIU*, 110:281–307, 2007.
- [6] CASIA databases. <http://biometrics.idealtest.org/>.
- [7] H.-Y. Chen, S.-Y. Chien. Eigen-patch: Position-patch based face hallucination using eigen transformation. *Proc ICME*, 2014.
- [8] J. Daugman. How iris recognition works. *IEEE TCSVT*, 14:21–30, 2004.
- [9] A. Deshpande, P. P. Patavardhan, D. H. Rao. Super-resolution for iris feature extraction. *Proc ICCIC*, 2014.
- [10] H. Hofbauer, F. Alonso-Fernandez, P. Wild, J. Bigun, A. Uhl. A ground truth for iris segmentation. *Proc ICPR*, 2014.
- [11] A. Jain, P. Flynn, A. Ross, editors. *Handbook of Biometrics*. Springer, 2008.
- [12] A. K. Jain, A. Kumar. *Second Generation Biometrics*, chapter Biometrics of Next Generation: An Overview. Springer, 2010.
- [13] J. Jiang, R. Hu, Z. Wang, Z. Han. Face super-resolution via multilayer locality-constrained iterative neighbor embedding and intermediate dictionary learning. *IEEE TIP*, 23(10):4220–4231, Oct 2014.
- [14] D. Jobson, Z.-u. Rahman, G. Woodell. A multiscale retinex for bridging the gap between color images and the human observation of scenes. *IEEE TIP*, 6(7):965–976, 1997.
- [15] F. Juefei-Xu, M. Savvides. Subspace-based discrete transform encoded local binary patterns representations for robust periocular matching on nist face recognition grand challenge. *IEEE TIP*, 23(8):3490–3505, 2014.
- [16] D. Lowe. Distinctive image features from scale-invariant key points. *IJCV*, 60(2):91–110, 2004.
- [17] L. Masek. Recognition of human iris patterns for biometric identification. Master’s thesis, School of Computer Science and Software Engineering, University of Western Australia, 2003.
- [18] K. Nguyen, S. Sridharan, S. Denman, C. Fookes. Feature-domain super-resolution framework for gabor-based face and iris recogn. *Proc CVPR*, 2012.
- [19] I. Nigam, M. Vatsa, R. Singh. Ocular biometrics: A survey of modalities and fusion approaches. *Information Fusion*, 26, 2015.
- [20] S. C. Park, M. K. Park, M. G. Kang. Super-resolution image reconstruction: a technical overview. *IEEE SPM*, 20(3):21–36, 2003.
- [21] G. W. Quinn, P. Grother, M. Ngan. IREX IV: Pt 2 - compression profiles for iris image compress. *NISTIR 7978* - <http://www.nist.gov/itl/fiad/ig/irexiv.cfm>, 2014.
- [22] C. Rathgeb, A. Uhl. Secure iris recognition based on local intensity variations. *Proc ICIAR*, 2010.
- [23] K. Y. Shin, K. R. Park, B. J. Kang, S. J. Park. Super-resolution method based on multiple multi-layer perceptrons for iris recognition. In *Proc ICUT*, 2009.
- [24] V. Štruc, N. Pavešić. Gabor-based kernel partial-least-squares discrimination features for face recognition. *Informatica (Vilnius)*, 20(1):115-138, 2009.
- [25] V. Štruc, N. Pavešić. *Advances in Face Image Analysis: Techniques and Technologies*, chapter Photometric normalization techniques for illumination invariance, pp. 279–300. IGI Global, 2011.
- [26] N. Wang, D. Tao, X. Gao, X. Li, J. Li. A comprehensive survey to face hallucination. *IJCV*, 106(1):9–30, 2014.
- [27] K. Zuiderveld. Graphics gems iv. pp. 474–485, 1994.